Nuclear Inst. and Methods in Physics Research B 466 (2020) 12–16

Contents lists available at ScienceDirect

Nuclear Inst. and Methods in Physics Research B

journal homepage: www.elsevier.com/locate/nimb

Phenomenology of the effect of ion irradiation on the work function of metals

Ákos Horváth, Norbert Nagy, Gábor Vértesy, Robert Schiller*

Centre for Energy Research, P.O. Box 49, Budapest 1525, Hungary

ARTICLE INFO

Keywords:
Electron work function
Simple metals
Ion irradiation
Wigner-Seitz radius
Annealing

ABSTRACT

Polycrystalline Al and Zn samples were irradiated with 30 keV Ar^+ ions at room temperature and the changes of their electron work functions, Φ were measured by the Kelvin method. Similarly to what was earlier experienced with stainless steel the changes of Φ as a function of displacement per atom (DPA) were seen to be of extremal character. This can be considered as a manifestation of competing formation and annealing of displacements. Comparing the Lang-Kohn theory of work function with the present experimental results the changes of the Wigner-Seitz radii were evaluated. A differential law for the dependence of the Wigner-Seitz radius on DPA is proposed.

1. Introduction

The effect of accelerated ions on metals, studied in a number of fields and in many different aspects, is also of considerable practical importance in nuclear technology. Throughout the operation of a nuclear power station its structural materials are exposed to neutron irradiation which greatly influences their properties with important consequences as far as mechanical reliability or corrosion resistance are concerned. With an increasing number of power stations coming to an age the study of those processes has become demanding. Obviously, the practical problems require a number of basic phenomena to be treated.

Any experimental work which directly simulates the radiation conditions of a working reactor is, however, most cumbersome. Neutron irradiation makes the substances radioactive hence the handling of the samples is difficult. Usually several years are needed for the activities to decrease to a safe level and/or complicated radiation shields and remote controlled equipment must be used. In order to avoid these difficulties the metals to be investigated are often exposed to a flux of accelerated ions instead of reactor neutrons.

This replacement is far from being obvious in view of the differences between neutrons and ions as far as penetration depths in, and modes of interaction with the target are concerned [1]. However, the use of accelerated ions is advantageous not only in view of lower costs and the practical absence of radioactivity but also it enables one to vary irradiation conditions easily also by changing the nature of the projectile [2].

The introduction of the variable called displacement per atom (DPA) instead of fluence removes a good part of the problems which stem from the great variety of interactions between target and radiation [1]. Let A denote the number of atoms in unit volume of the sample, $I(E)$ the flux of particles of energy E, E_{max} and E_{min} the maximum and minimum energy in the particle beam, respectively, and $\sigma_D(E)$ the cross section of displacement of an atom in the target. The number of displacements per unit volume and unit time, R is given by the equation

$$R = A \int_{E_{min}}^{E_{max}} I(E)\sigma_D(E)dE \tag{1}$$

Giving the total number of displacements per unit volume as $D = Rt$ after irradiation period, t, DPA is defined as

$$\mathrm{DPA} = N = \frac{D}{A} \tag{2}$$

N will be used as the symbol for DPA in the mathematical expressions.

The displacement cross section can be evaluated in terms of the particle-lattice interactions scenario. As the first stage the incident particle hits an atom imparting an energy K which is usually beyond the atom's binding energy. Thereafter the primary knock-on atom (PKA) hits further lattice atoms displacing them at the expense of its extra energy. Let $\sigma(E, K)$ denote the cross section of the process in the course of which PKA obtains energy K from a projectile of energy E and let $n(K)$ be the number of atoms displaced by the PKA. The displacement cross section, $\sigma_D(E)$ is then given as

$$\sigma_D(E) = \int_{K_{min}}^{K_{max}} \sigma(E, K)n(K)dK \tag{3}$$

* Corresponding author.
E-mail address: schiller.robert@energia.mta.hu (R. Schiller).

https://doi.org/10.1016/j.nimb.2020.01.004
Received 26 November 2019; Accepted 6 January 2020

Detailed calculations were carried out both for $\sigma(E, K)$ and $n(K)$ for different projectiles and different lattices with a number of distinct modes of projectile-lattice interaction [3]. By making use of these results DPA can be evaluated in terms of Eqs. (1)–(3). Experience has shown that the experimental data treated as a function of DPA depend but little on either the energy or the nature of the accelerated particles [3].

Majority of the research in this field has referred to the variation in mechanical properties and in the microscopic structures of the irradiated metals. Since alloys are the most commonly used construction materials the processes of segregation and recrystallization have deserved great attention. Corrosion studies or investigations with direct electrochemical relevance have been carried out comparatively rarely, with the important exception of stress corrosion cracking (a short summary on earlier research is given in our previous publications [4,5]).

The above description regards the irradiated solid sample as a homogeneous system neglecting any spatial correlation of the elementary acts [6]. This approach seems to be sufficient for the understanding of the final, post-irradiation conditions. The description of fast kinetics, however, must involve also local and temporal inhomogeneities, i.e. ion tracks. This idea, first introduced by Jaffé [7] and modified by Dessauer [8], who proposed point heat as the primary source of local events, has taken shape more recently as thermal spike theory [9]. This is regarded as the most general approach upon which track kinetics can rest [10]. Kinetic problems, however, will not be dealt with in the forthcoming parts of this paper the treatment being kept at the phenomenological level of the post-irradiation conditions.

Normal electrode potential of a metal is known to be a monotonous function of its electron work function [11,12], whereas the difference between the work functions of two metals is equal with the difference of their standard electrode potentials [13,14]. One would expect this linear relationship to prevail particularly strictly if the irradiated and virgin states of one and the same metal are compared.

Beyond the electron work function, hence the normal electrode potential, several other material properties of metals are also known to depend directly on the Fermi energy: like electron heat capacity, cohesive energy, bulk modulus, and thermal expansion [15]. The practically important interrelation between work function and mechanical properties were substantiated both experimentally [16–20] and theoretically [21].

The electron work function has been theoretically described by Lang and Kohn [22] as the difference between $\delta\varphi$, the mean electrostatic potential drop across the metal surface, and μ, the bulk chemical potential of the electrons (Fermi energy) as

$$\Phi^{theor} = \delta\varphi - \mu \tag{4}$$

The theory is based on a jellium model where the wave number of the electron is inversely proportional to the Wigner-Seitz radius of the metal, r_s. Both quantities on the right hand side are the sole functions of r_s. Lang and Kohn presented the theoretical results in numerical form, we could fit simple exponential functions to their data as

$$\delta\varphi(r_s) = \delta\varphi_0 + A_\varphi e^{-r_s/\sigma_\varphi} \tag{5}$$

$$\mu(r_s) = \mu_0 + A_\mu e^{-r_s/\sigma_\mu} \tag{6}$$

Theoretical points and fitted curves are given in Fig. 1.

Earlier, in order to get some insight into the effect of irradiation on the electrochemistry of stainless steel, we studied the variation of its electron work function by bombardment with fast Ar^+ and H^+ ions [5]. The metal studied was the construction material of the Hungarian nuclear power station, Paks, Type AISI 321. The most striking result was the extremal nature of the change of work function with DPA: at low DPA the work function was seen to increase, it attained a maximum and then it decreased.

The present study was prompted by that finding. We wanted to investigate whether the extremal behaviour of the work function versus DPA can be observed also with other metals. Instead of an alloy, like stainless steel, we chose two simple metals, Al and Zn, for these experiments.

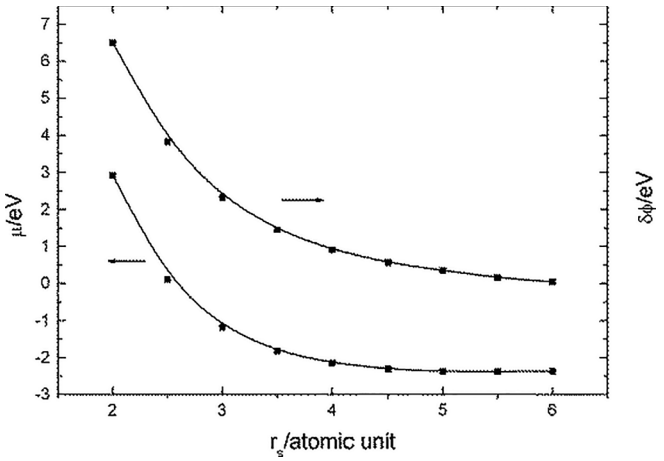

Fig. 1. Theoretical results by Lang and Kohn[15] (dots) together with fitted curves[5] (lines), according to Eqs. (5) and (6) with fitting parameters $\delta\varphi_0 = 0.0035$; $A_\varphi = 49.0$; $\sigma_\varphi = 0.99$; $\mu_0 = -2.42$; $A_\mu = 102$; $\sigma_\mu = 0.68$.

As before, we measured electron work function by making use of the Kelvin method [23–27]. This was chosen because it does not require high vacuum and high temperature in contrast to methods based on photo effect or thermionic emission [28]. Thus the metal surface can be measured at room temperature and atmospheric conditions without running the risk of changing the state of the surface which is normally exposed to the environment. The disadvantage of the method is that it informs only about the difference between the work functions of two metals one of them being the sounding tip of the instrument. However, since the aim of our study was to reveal *changes* of the work function, this limitation is immaterial.

2. Experimental

2.1. Materials

Al ribbon of p.a. purity, with 0.3 mm thickness, Merck, and Zn foil of 99.99% purity with 1 mm thickness, Advent, were used in the form of 10mmx10mm pieces. Before and after irradiation the samples were sonicated in iso-propanol for one hour, dried in laboratory atmosphere and kept overnight in the Faraday box of the Kelvin probe.

2.2. Irradiation

Details of facility and conditions are described in the earlier paper [5]. 30 keV Ar^+ ions with a current density of 0.4 μA/cm^2 were used with fluences of 5.2, 7.8, 13, 16, 25, 31, 36, 45, 50 × 10^{14} cm^{-2} for the Al, and 3.4, 5.7, 7.0, 11.5, 13.5, 16, 18, 20.5, and 27.5 × 10^{14} cm^{-2} for the Zn samples. The incident beam was made to sweep over the sample so as to make the flux uniform over the surface to at least 98 percent. The temperature of the sample did not increase practically throughout irradiation. One half of each sample was covered and the other half irradiated the unirradiated portion serving as the virgin sample for comparison.

2.3. DPA calculation

The depth distribution of DPA was evaluated *via* full-cascade Monte-Carlo simulation for at least 10,000 ions using the SRIM software [29]. The normalized areas of the DPA peaks were calculated by integrating the DPA *versus* depth curve in the range of full width at half maximum

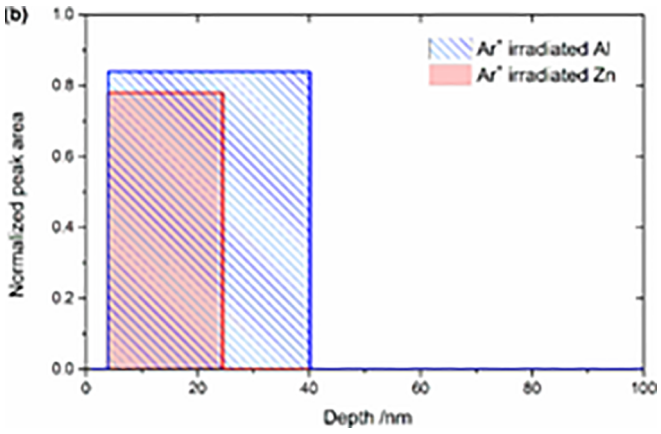

Fig. 2. Depth distributions of DPA by 30 keV Ar^+ ions in Al and in Zn, as computed by Eq. (7).

according to Eq. (7) where x_c denotes the depth of the maximum and $(x_1 + x_2)$ equals the full width at half maximum,

$$Normalized\ \ peak\ \ area = \frac{\int_{x_c-x_1}^{x_c+x_2} DPA(x)dx}{\int_0^{\infty} DPA(x)dx} \tag{7}$$

The results for the two metals are given in Fig. 2 and in Table 1

2.4. Measurements

Work function was measured by the Ambient Kelvin Probe of KP Technology [16] equipped with a sample positioning system developed by Plósz Engineering Co. Ltd. Relative measurements were performed determining the work function differences between the irradiated and virgin portions of the samples. Ten different positions having usually been measured on both portions averages and standard deviations were evaluated.

3. Results and discussion

The measured changes of work function, $\Delta\Phi^{exp}$ of Al and Zn are given in Figs. 3 and 4. The fitted curves, similar to our earlier results referring to stainless steel [5], are Lorentz functions, Eq. (8),

$$\Delta\Phi^{exp} = \Delta\Phi_0 + \frac{A}{\pi}\frac{\sigma}{1 + (N - N_c)^2{\sigma_{exp}}^2} \tag{8}$$

here N denotes DPA further symbols being fitting parameters. Given the error limits and the limited number of data points the numerical values of the fitting parameters are of minor importance, hence no error limits of the parameters are given. The only exception is N_c which was found to be around 8 with an error of about 8% for both metals. Nevertheless, considering Figs. 3 and 4, together with the earlier finding on steel, we think that Lorentz function describes the observations reasonably well. Its physical content will be interpreted later.

The questions formulated in the Introduction can be answered now. $\Delta\Phi$, as a function of DPA, has an extremum both for Al and Zn, similar to the observations on steel.

As it is shown in Fig. 2 and Table 1. the majority of Ar^+ ions

Table 1
Data of calculated DPA distributions of the Ar^+-irradiated Al and Zn samples.

	Al	Zn
x_c/nm	36.2	20.7
x_1/nm	15.57	8.26
x_2/nm	20.64	12.44
Normalized peak area	0.84	0.78

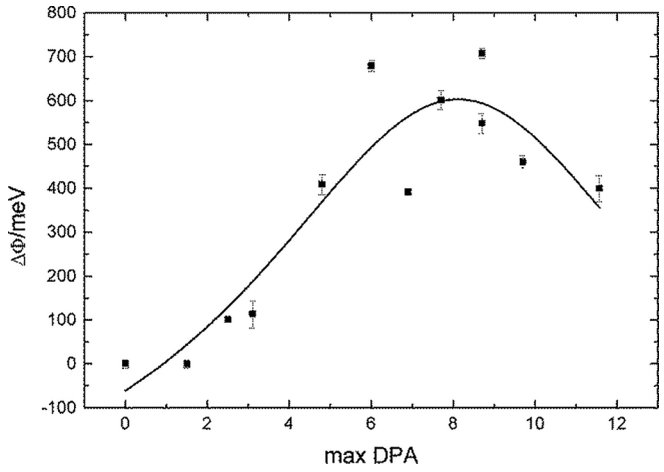

Fig. 3. Work function change, $\Delta\Phi^{exp} = \Phi(irradiated) - \Phi(virgin)$ of polycrystalline Al by 30 keV Ar^+ irradiation as a function of max. DPA. Curve fitted according to Eq. (8), fitting parameters: $\Delta\Phi_0 = -451.6$; $N_c = 8.12$; $\sigma_{exp} = 0.160$; $A = 20662$. Error limits of the parameters are deliberately omitted, see text.

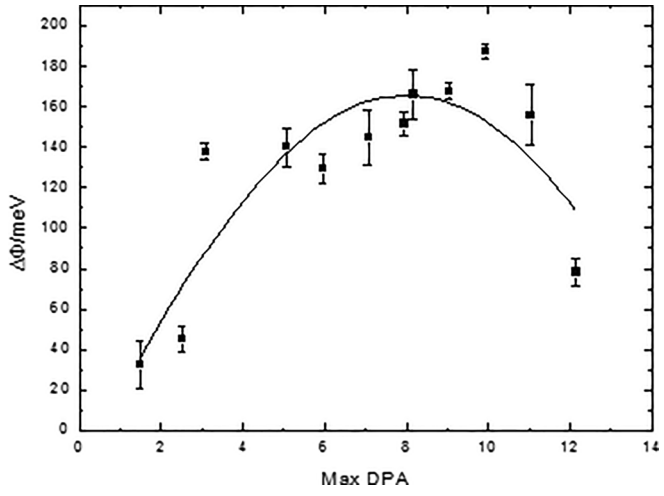

Fig. 4. Work function change, $\Delta\Phi^{exp} = \Phi(irradiated) - \Phi(virgin)$ of polycrystalline Zn by 30 keV Ar^+ irradiation as a function of max. DPA. Curve fitted according to Eq. (8), fitting parameters: $\Delta\Phi_0 = -1128$; N_c=7.99; $\sigma_{exp} = 0.0514$; $A = 79148$. Error limits of the parameters are deliberately omitted, see text.

penetrates to a depth of several nanometres below the geometrical surface both into Al and Zn. Hence it seems reasonable to attribute the effects of radiation mainly to bulk processes in both cases. Thus, as a first approximation, it is only μ that is influenced by the impinging ions, hence theory describes the change of the work function, $\Delta\Phi^{theor}$ as

$$\Delta\Phi^{theor}(r_s) = -[\mu(r_s^{'}) - \mu(r_s)] = A_\mu e^{-r_s/\sigma_\mu}(1 - e^{-\Delta r_s/\sigma_\mu}) \cong A_\mu e^{-r_s/\sigma_\mu}\frac{\Delta r_s}{\sigma_\mu} \tag{9}$$

here $\Delta r_s = r_s^{'} - r_s$ where $r_s^{'}$ is the Wigner-Seitz radius in the irradiated sample and r_s that in the virgin one.

By setting $\Delta\Phi^{theor} = \Delta\Phi^{exp}$ one can evaluate Δr_s as a function of N as it is expressed by Eq. (10),

$$\Delta r_s = -\sigma_\mu ln\left(1 - \frac{\Delta\Phi^{exp}(N)}{A_\mu e^{-r_s/\sigma_\mu}}\right) \cong \sigma_\mu \frac{\Delta\Phi^{exp}(N)}{A_\mu e^{-r_s/\sigma_\mu}} \tag{10}$$

By making use of the appropriate theoretical parameters and observed data for Al and Zn, respectively, Figs. 5 and 6 are obtained.

The change of the Wigner-Seitz radius, Δr_s is positive in the entire range studied. The most striking feature of Figs. 5 and 6 is their

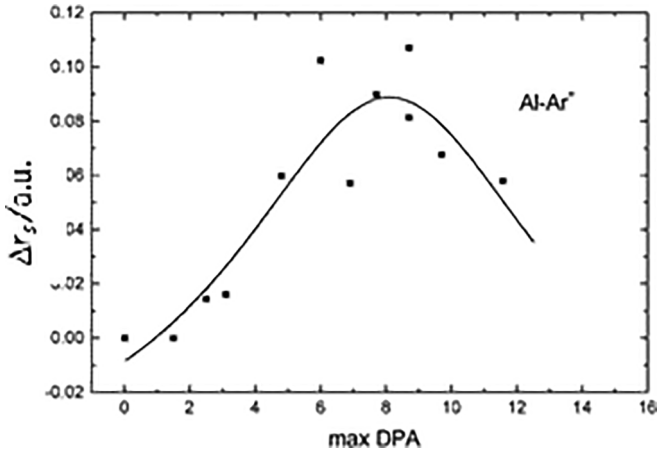

Fig. 5. Dependence of the variation of the Wigner-Seitz radius on DPA in Al upon Ar^+ irradiation evaluated according to Eq. (10). Error limits are proportional to those in Fig. 4, continuous line calculated from the fitted curve.

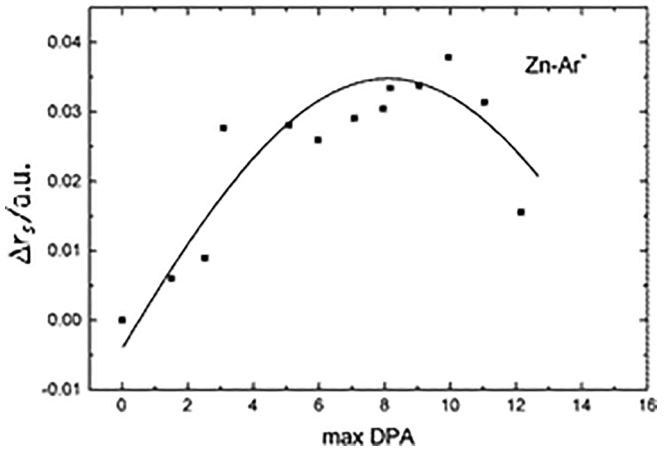

Fig. 6. Dependence of the variation of the Wigner-Seitz radius on DPA in Zn upon Ar^+ irradiation evaluated according to Eq. (10). Error limits are proportional to those in Fig. 5, continuous line calculated from the fitted curve.

extremal nature. The Wigner-Seitz radii of both metals increase at low DPA, reach a maximum at about $N_c = 8$ then decrease again.

This phenomenon seems to be a manifestation of radiation annealing, a phenomenon described earlier from several aspects. D.C. resistivities of copper, silver and gold as a function of fluence were seen to have maxima [30]. The variation of channeling linewidth with fluence indicated the annealing of the dislocation network in self-ion irradiated aluminium[31]. Pre-existing defects in SiC were annealed by ionizing radiation [32]. As far as technically important alloys are concerned the embrittlement of reactor steel [33] and the ductility of an aluminium alloy [34] were seen to reveal radiation annealing. Radiation-effected annealing in a nickel-based alloy was attributed to the reduction of intrinsic dislocation density due to radiation action [35]. An extremum as a function of DPA was indicated in the lattice distortion of GH3535 alloy weld metal [36]. Theoretical interpretations were proposed by Averback and Diaz de la Rubia [37] and Na-Young Park et al. [38].

The present study may be paralleled with the determination of Fermi level shifting by ion irradiation in doped anatase films [39]. The important difference between irradiated semiconductors and single component metals can be expressed in terms of the the energy band structure. Whereas in a semiconductor irradiation influences the band structure, in a pure metal the band structure remains unchanged and only the chemical potential of the electron ensemble (the Ferni energy) is influenced by ion bombardment.

In order to formulate the above results analytically the inverse Fourier transform of the fitted Lorentz function, Eq. (7) is used, writing

$$F^{-1}(\Delta\Phi^{exp}(N) - \Delta\Phi_0) = \Delta\Phi^{exp}(\nu) = A_{exp}e^{-(\nu-\nu_c)/\sigma_{exp}} \tag{11}$$

with $\nu = 1/N$ and $\nu_c = 1/N_c$.

The theoretical expression for the change in the work function is given by Eq. (9). Again let us equate the theoretical expression with the fitted experimental curve, now as a function of ν,

$$\Delta\Phi^{exp}(\nu) = \Delta\Phi^{theor}(r_s) \tag{12}$$

By making use of Eq. (11), and of the approximate formula in Eq. (9), Δr_s can be expressed. After derivation with respect to ν one finds

$$\frac{dr_s}{d\nu} = \frac{\sigma_\mu}{\sigma_{exp}}\frac{\Delta\Phi^{exp}(\nu)}{\mu(r_s) - \mu_0} \tag{13}$$

This equation expresses the rate of variation of the Wigner-Seitz radius as a function of the reciprocal of DPA. The experimental data, given by $\Delta\Phi^{exp}(\nu)/\sigma_{exp}$, are related to the theoretical function, $\mu(r_s)/\sigma_\mu$,which refers to the virgin sample. The latter can be obtained from Eq. (6) once the metal's initial Wigner-Seitz radius is known.

The variable ν can be visualized by the following consideration. By definition ν is given as $\nu = A/D$ using the notation of Eq. (2). Since the number of particles per unit volume, i.e. the number density, is the reciprocal of the volume per particle, $A = 3/4\pi r_s^3$ and $D = 3/4\pi r_d^3$ one can write

$$\nu = \frac{r_d^3}{r_s^3} \tag{14}$$

The half distance between two neighboring displacements is $r_d = r_s\sqrt[3]{\nu}$.

At $\nu = \nu_c$ the exponent in Eq. (11) changes sign and the abscissae of the maxima in Figs. 3–6 equals$1/\nu_c = N_c$. If one attributes the change of r_s to the presence of dislocations, this observation can be interpreted in the following manner. Formation and disappearance of displacements are competing processes throughout irradiation, at $N \geq N_c$ disappearance outdoes formation. The limiting PDF value defines a critical distance between neighboring displacements, r_d^c in terms of Eq. (14). Half of the critical distance between two displacements at N_c is

$$r_d^c = r_s\sqrt[3]{\nu_c} \tag{15}$$

Present measurements rendered $N_c \cong 8$ both for Ag and Zn. Hence in these two cases one finds for the average critical distance between neighboring displacements to be $2r_d^c \cong r_s$. Disappearance of displacements becomes overwhelming if the displacements are nearer to each other than the Wigner-Seitz radius. Only further measurements could tell whether this finding holds also for other simple metals.

4. Conclusions

Electron work function, Φ is closely related to the electrochemical behavior of metals, and also to several other, mechanical and thermal properties. The aim of the present research was to investigate the effect of particle irradiation on work function. That question was prompted by the radiation damage of the construction materials in nuclear reactors. Simple metals, Al and Zn, were irradiated with 30 keV Ar^+ ions at room temperature. The work function was seen to increase with increasing DPA (displacement per atom), N, to reach a maximum at N_c and then to decrease but to remain always larger than that of the virgin metal. The extremal $\Phi(N)$ curve is thought to manifest the competing formation and annealing of displacements. The present observations are in keeping with our earlier findings on stainless steel.

Comparing the experimental results with the theory of Lang and Kohn the observations could be interpreted in terms of the Wigner-Seitz radii of the metals. The irradiation-effected variatons of the radii were

evaluated and also a differential expression for the variation as a function of $\nu = 1/N$, was suggested. One can visualize ν as the volume per DPA divided by the volume of the Wigner-Seitz sphere.

We hope that the present phenomenology might serve as a basis to reveal some further aspects of the elementary steps of radiation action.

Declaration of Competing Interest

The authors declare that they have no known competing financial interests or personal relationships that could have appeared to influence the work reported in this paper.

References

[1] G.S. Was, Challenges to the use of ion irradiation for emulating reactor irradiation, J. Mater. Res. 30 (2015) 1158–1182.
[2] N.H. Packan, K. Farrell, J.O. Stiegler, Correlation of neutron and heavy-ion damage: I. The influence of dose rate and injected helium on swelling in pure nickel, J. Nucl. Mater. 78 (1978) 143–155.
[3] G.S. Was, Fundamentals of Radiation Material Science, Springer, Berlin, 2007.
[4] Á. Horváth, N. Nagy, R. Schiller, Particle irradiation and electron work function: Fe single crystal bombarded with Ar+ ions, Radiat. Phys. Chem. 124 (2016) 38–40.
[5] Á. Horváth, N. Nagy, G. Vértesy, R. Schiller, The effect of ion irradiation on the electron work function of stainless steel, Mater. Chem. Phys. 217 (2018) 541–546.
[6] K. Gärtner, Ion-solid interaction, in: Werner Wesch, Elke Wendler (Eds.), Ion Beam Modification of Solids: Ion-Solid Interaction and Radiation Damage, Springer, AG Switzerland, 2016, pp. 3–62.
[7] G. Jaffé, Zur theorie der ionisation in kolonnen, Ann. Phys. 42 (1913) 303.
[8] F. Dessauer, Über einige Wirkungen von Strahlen, Z. Phys. 20 (1923) 288–298.
[9] A. Kamarou, W. Wesch, E. Wendler, A. Undisz, Retlenmayr, Swift heavy ion irradiation of InP: thermal spike modeling of track formation, Phys. Rev. B 73 (2006) 184107.
[10] C. Dufour, M. Toulemonde, Models for the description of track formation, in: Werner Wesch, Elke Wendler (Eds.), Ion Beam Modification of Solids: Ion-Solid Interaction and Radiation Damage, Springer, AG Switzerland, 2016, pp. 63–104.
[11] S. Trasati, The electrode potential, in: J.O'M. Bockris, B.E. Conway, E. Yaeger (Eds.), The Electrode Potential, Plenum Press, New York, 1980, pp. 45–81T.
[12] J. Goodisman, Electrochemistry: Theoretical Foundations, Wiley, New York, 1987.
[13] J.O'M. Bockris, S.U.M. Khan, Surface Electrochemistry, Plenum Press, New York, 1993.
[14] W. Schmickler, E. Santos, Interfacial Electrochemistry, second ed., Springer, Heidelberg, 2010.
[15] S.R. Elliott, The Physics and Chemistry of Solids, Wiley, Chichester, 1998.
[16] R. Rahemi, Dongyang Li, Variation in electron work function with temperature and its effect on the Young's modulus of metals, Scr. Mater. 99 (2015) 41–44.
[17] Guomin Hua, Dongyang Li, Electron work function: a novel probe for toughness, Phys. Chem. Chem. Phys. 18 (2016) 4753–4759.
[18] Lu. Hao, Guomin Hua, Dongyang Li, Dependence of the mechanical behavior of alloys on their electron work function—an alternative parameter for materials design, Appl. Phys. Lett. 103 (2013) 261902.
[19] Lu. Hao, Ziran Liu, Xianguo Yan, Dongyang Li, L.E. Parent, Harry Tian, Electron work function–a promising guiding parameter for material design, Sci. Rep. 6 (2016) 24366.
[20] Z.D. Han, Y.Z. Guan, W. Li, X.Y. Zhang, Mechanical properties and work function of L21 structure AlCu2X (X = Ti, Mn, Zr, or Hf) intermetallics, Mater Sci. Eng. A 545 (2012) 13–19.
[21] Shuai Zhang, Cher Ming Tan, Shuguang Cheng, Tianqi Deng, Feifei He, Su Haibin, Ab initio simulation of electronic and mechanical properties of aluminium for fatigue early feature investigation, Int. J. Nanotechnol. 11 (2014) 373–385.
[22] N.D. Lang, W. Kohn, Theory of metal surfaces: work function, Phys. Rev. B 3 (1971) 1215–1223.
[23] Lord Kelvin, Contact electricity of metals, Phil. Mag. Series 5 46 (278) (1898) 82–120.
[24] J. Jäckle, The origin of the thermoelectric potential 2000 http://www.uni-konstanz.de/FuF/Physik/Jaeckle/papers/thermopower/thermopower.html.
[25] Ambient Kelvin Probe, Hardware and Software Manual 2014, KP Technology, pp. 1–30.
[26] Antoine Kahn, Fermi level, work function and vacuum level, Mater. Horiz. 3 (2016) 7–10.
[27] Rudy Schlaf, Tutorial on Work Function http://rsl.eng.usf.edu/Document/Tutorials/TutorialsWorkFunction.pdf.
[28] I.F. Patai, M.A. Pomerantz, Contact potential differences, J. Franklin Inst. 252 (1952) 239–260.
[29] J.M. Ziegler, 2013, http://www.srim.org.
[30] R.S. Averback, K.L. Merkle, Radiation-annealing effects in energetic displacement cascades, Phys. Rev. B 16 (1977) 3860–3869.
[31] R.G. Wardiman, The formation and annealing of dislocation damage from high-dose self-ion implantation of aluminum, J. Appl. Phys. 71 (1992) 5386–5390.
[32] Y. Zhang, et al., Ionization-induced annealing of pre-existing defects in silicon carbide, Nat. Commun. 6 (2015) 8049.
[33] E. Krasikov, V. Nikolaenko, Radiation annealing of radiation embrittlement of the reactor pressure vessel steel, IOP Conf. Series: Mater. Sci. Eng. 110 (2016).
[34] V.V. Ovchinnikov, N.V. Gushchina, S.M. Mozharovsky, L.I. Kaigorodova, Low-temperature volume radiation annealing of cold-worked bands of Al-Li-Cu-Mg alloy by 20–40 keV Ar+ ion, IOP Conf. Series, Mater. Sci. Eng. 168 (2017) 012067.
[35] H.C. Chen, D.H. Li, R.D. Lui, H.F. Huang, J.J. Li, G.H. Lei, Q. Huang, L.M. Bao, L. Yan, X.T. Zho, Z.Y. Zhu, Nucl. Instrum. Meth. Phys. Res. Sect. B 377 (2016) 94–98.
[36] Hefei Huang, Xiaoling Zhou, Chaowen Li, Jie Gao, Tao Wei, Guanhong Lei, Jianjian Li, Linfeng Ye, Qing Huang, Zhiyong Zhu, Temperature dependence of nickel ion irradiation damage in GH3535 alloy weld metal, J. Nucl. Mater. 497 (2017) 108–116.
[37] R.S. Averback, T. Diaz de la Rubia, Displacement damage in irradiated metals and semiconductors, in: H. Ehrenreich, F. Spaepen (Eds.), Solid State Physics, vol. 51, Academic Press, San Diego, 1998, pp. 282–402.
[38] Na-Young Park, Yu-Chan Kim, Hyun-Kwang Seok, Seung-Hee Han, Seungyon Cha, Pil-yung Cha, Molecular dynamics simulation of irradiation damage in tungsten, Nucl. Instrum. Methods Phys. Res. Sect. B 265 (2007) 547–552.
[39] S.K. Gautham, A. Das, S. Ojha, D.K. Shukta, D.M. Phase, F. Singh, Electronic structure modification and Fermi level shifting in niobium-doped anatase titanium dioxide thin films: a comparative study of NEXAFS, work function and stiffening of phonons, Phys. Chem. Chem. Phys. 18 (2016) 3618–3627.